Study of Cyclic Voltammetry Behaviour of Transition Metal Dopant in Magnesium Ferrites

Erdawati[1], Yusmaniar[2] and Rita Sundari[3,*]

[1]Master of Chemistry Education, State University of Jakarta, DKI Jakarta 13220, Indonesia
[2]Department of Chemistry, State University of Jakarta, DKI Jakarta 13220, Indonesia
[3]The Research Center of Private Universities Coordination, 13360 Jakarta, Indonesia

*Corresponding author:E-mail: ritsun2003@yahoo.com; erda_wati_0912@yahoo.com

The cyclic voltammetry of magnesium ferrites ($Mg_{1-x}Fe_2O_4$) plays important role as a primary investigation in relation to its electrochemical properties. This investigation has been encountered with the study of cyclic voltammetry of metal dopant (Mn, Co and Ni) magnesium ferrites. The doped and undoped magnesium ferrites were synthesized by a sol gel method using polyvinyl alcohol and citric acid mixed and stirred at 80 °C for 5 h. The gel products were calcined at 500-900 °C. Anautolab PGSTAT 30 interface coupled with a processor using a general purpose electrochemical system (GPES) software was applied to present the cyclic voltammetry. The mixture of fabricated doped or undoped ferrites and poly(vinylidene fluoride) (PVDF) deposited on a screen printed carbon electrode (SPCE) as the working electrode was dipped into a mixture of phosphate buffer and ferricyanide solution in the electrochemical system. The cyclic voltammetry curves were recorded applying a scan rate of 0.02 V s^{-1}.

Keywords: Cyclic voltammetry, Metal dopant, Magnesium ferrites, SPCE.

INTRODUCTION

Magnesium ferrite ($MgFe_2O_4$) and its metal dopant show good properties for semi conducting materials in relation to their cubic structures, chemical and thermal stabilities[1]. The spinel structure of $MgFe_2O_4$ with the Mg^{2+} and Fe^{3+} ions occupy either the tetrahedral or octahedral sites and the oxygen atoms form the face-centered cubic is supposed to contribute the electrical conducting properties[2]. To date, magnesium ferrites have attracted great interest because of their broad applications in sensors, heterogeneous catalysts, electrical and magnetic materials. For the basic study of electrochemistry, the cyclic voltammetry technique was commonly used because it involves with the redox behaviour in electrochemical properties. Several investigations in relation to cyclic voltammetry characteristics were reported such as, the study of corrosion effects in electro-deposited Zn-Ni alloy from sulfate solution, the examination of superoxide ion generation from trihexylphosphoniumimide ionic liquid, the oxidation process of ascorbic acid using multi-walled carbon nanotubes (MWCNT)/TiO_2 composite attached to glassy carbon electrode, the electrochemical study of nickel complexes with sulphonylhydrazone, the electrochemical reaction of omeprazole using glassy carbon electrode, the study of cyclic voltammetry and differential pulse voltammertry (DPV) of fluvastatin sodium using glassy carbon electrode

and the cyclic voltammetry characterization of pyrrole poly-merization using platinum electrode coated with nafion dopant[3-6]. Based on this reason, this work decided to investigate the cyclic voltammetry study of magnesium ferrites and its metal doping (Mn, Co and Ni) as the primary investigation in relation to its electrochemical properties.

A lot of synthesis methods of ferrites have been previously investigated to produce better semiconducting properties, such as coprecipitation, electrospinning, solid state reaction, sol gel, self combustion, oxidative thermal decomposition and high energy ball milling treatment[7,8].

Among the various methods of fabrication, the sol gel method was more reasonable for the synthesis of ferrites in terms of low temperature, homogeneous product and particle size distribution[9,10]. On other occasions, the sol gel method was also chosen in the synthesis of ZnO-Al for thin film coating and ZnO-carbon nanotubes-PVA composite for electromagnetic detector because of process simplicity and easy control of the film composition[11,12]. Therefore, this study chose the sol gel method for the synthesis of magnesium ferrites and its dopant metals of interest (Mn, Co and Ni)followed by calcinations under high temperatures (500-900 °C).

Previous investigation showed that a metal dopant in a material of interest can enhance the desired properties of that material. Arsana *et al.*[13] used silver and copper doped zinc

oxide to enhance the photodegradation effect on dyes under visible light, while Benouis *et al.*[14] studied the photoconductivity effect of aluminum and indium doped zinc oxide thin film. Puspitasari *et al.*[8] applied manganese doped zinc ferrite to improve the mechanical strength for catalyst application. In other work, the effects of various concentrations of Ni and Al dopants in magnesium ferrites were studied to optimize the ceramic properties of ferrite material[15,16].

To the best of our knowledge, the study on metals dopant ferrites and other metallic materials were concentrated on the method of synthesis and characterization studies mostly applied Fourier transformation infrared (FTIR), X-ray diffraction (XRD), ultra violet diffuse reflectance (UVDR) and scanning electron microscope methods[9-16]. Herein, we wish to expose the study of cyclic voltammetry behaviour of magnesium ferrites and its metals dopant (Mn, Co and Ni) and FESEM-EDX analysis for the characterization study. For the cyclic voltammetry study, we used own fabricated magnesium ferrite and its metal dopant deposited on a screen printed carbon electrode (SPCE) as the working electrode in an amperometric method with a Ag/AgCl reference electrode and a glassy carbon counter electrode in an integrated system. We expected this study could produce satisfied results that would be valuable for the contribution of electrochemical properties of ferrite material.

EXPERIMENTAL

Analytical grade chemicals were used in this study including cobalt nitrate [$Co(NO_3)_2 \cdot 6H_2O$] was obtained from Emory. Nickel nitrate [$Ni(NO_3)_2 \cdot 6H_2O$], magnesium nitrate [$Mg(NO_3)_2 \cdot 6H_2O$], iron(III) nitrate [$Fe(NO_3)_3 \cdot 9H_2O$], potassium ferricyanide [$K_3Fe(CN)_6$ and hydrochloric acid (HCl, 37 % purity) were ordered from QRec, polyvinyl alcohol [$(-CH_2CH_2-)OH$]. Polyvinyl alcohol (PVA) and ethanol (C_2H_5OH, 95 % purity) were purchased from Fluka. Citric acid-monohydrate ($C_6H_8O_7 \cdot H_2O$) was ordered from Bendosen and disodium hydrogen phosphate-dihydrate ($Na_2HPO_4 \cdot 2H_2O$) was obtained from GCE.

Synthesis of magnesium ferrite: The synthesis of magnesium ferrite involved several steps: (i) magnesium(II) nitrate, iron(III) nitrate and citric acid were mixed and heated to 80 °C under continuous stirring, (ii) polyvinyl alcohol (PVA) was added to the mixture and continuously stirred at 80 °C for 5 h to obtain homogeneous solution, (iii) a transparent viscous gel was produced after 24 h stirring, (iv) an aluminum foil was applied to cover the top of the flask used for making sol gel and (v) an overnight drying in an oven was carried out to obtain a dried gel. A similar procedure was done for the metal doped (Co and Ni) magnesium ferrites, which the composition of the dopant metal was varied, *i.e.* x = 0.1, 0.5 and 0.9 for $M_xMg_{1-x}Fe_2O_4$ (M = Co and Ni). The ratio of M and Mg was based on molar concentration with respect to both elements. Citric acid was used as anionic surfactant to obtain a homogeneous solution[10]. Maensiri *et al.*[1] and Naseri *et al.*[17] used poly(vinyl pyrrolidone) (PVP) in the synthesis of ferrites as a capping agent to control the agglomeration of particles. Instead of PVP the present work used PVA for a similar reason.

The dried gel ferrite was crushed in a mortar and then heated in a muffle furnace. At the first stage of heating, the ferrite powder was fired at 200 °C for 2 h to remove all organic

matters. At the second step of heating, the ferrite was calcined in a muffle furnace. The undoped magnesium ferrite was calcined at varied temperatures (400, 500, 700 and 900 °C). The metal doped ferrite was calcined at 500 °C. The calcined product was ready to be used as the ferrite deposited on a screen printed carbon electrode (SPCE) as working electrode.

Cyclic voltammetry: The cyclic voltammetry was performed using a three electrode system at room temperature. Reguig *et al.*[18] used a three electrode system to perform cyclic voltammograms for the study of Ni(II) complexes. The modified screen printed carbon electrode (SPCE) as the working electrode was a fabricated magnesium ferrite (undoped or metal doped) and poly(vinylidene fluoride) dissolved in 5 μL ethanol deposited onto a carbon disc of a 4 mm diameter. The present work used a Ag/AgCl reference electrode and a glassy carbon counter electrode in an integrated system with the modified working electrode. In spite of a glassy carbon counter electrode, Reguig *et al.*[18] used a platinum wire as the counter electrode and a Ag/AgCl/KCl reference electrode provided with a salt bridge to perform cyclic voltammograms. A platinum sheet counter electrode and a Ag/AgCl/KCl reference electrode were also applied to study the corrosion effects in Zn-Ni alloy and the generation of superoxide ion at room temperature based on cyclic voltammograms[3,5]. The electrolyte consisted of 1 M KOH, 5.0 mM potassium ferricyanide and 1 M phosphate buffer placed in a 10 mL beaker glass. An autolab PGSTAT 30 coupled with a GPES software was applied to perform the cyclic voltammetry. Cyclic voltammograms were recorded between -0.5 V and +0.5 V with a scan rate of 0.02 V s^{-1}.

The cyclic voltammetry is strongly influenced by the kinetics of electrode processes, which the current is monitored as the potential of the electrode is changed[19]. Electrodes with strongly current-dependent potentials may produce concentration polarization and its contribution to the total over potential and it is called as the polarization over potential. Atkins and Paula[19] proposed the mechanism of electrode-electrolyte system as follows. The reduction $M^{z+} + ze^- \rightarrow M$ in a redox couple of the type M^{z+}, M is related to the Nernst eqn. 1. When the electrochemical cell is producing current, the ion concentration (c) with the electrode potential (E) is changed to (c') and the new electrode potential (E') is defined by eqn. 2. The change of ion concentration from c to c' in the Nernst diffusion layer produces a concentration gradient caused by a slow diffusion from the bulk solution to the electrode surface and becomes the rate determining step. The concentration over potential (η^c) is determined in eqn. 3. The concentration gradient through the Nernst diffusion layer is expressed by eqn. 4. The concentration gradient yields a flux of ions towards the electrode. According to the Fick's first law, the molar flux (J) is proportional to the concentration gradient as stated by eqn. 5. Thus, the particle flux towards the electrode can be determined from eqn. 6. The cathodic current density (j) towards the electrode is the product of particle flux and the charge transferred per mole of ions (zF) as stated by eqn. 7.

$$E = E^0 + \frac{RT}{zF} \ln c \qquad (1)$$

$$E' = E^0 + \frac{RT}{zF} \ln c' \qquad (2)$$

$$\eta^c = E' - E = \frac{RT}{zF} \ln \frac{c'}{c} \qquad (3)$$

$$\frac{dc}{dx} = \frac{c' - c}{\delta} \qquad (4)$$

$$J = -D \left(\frac{\partial c}{\partial x} \right) \qquad (5)$$

$$J = D \frac{c - c'}{\delta} \qquad (6)$$

$$j = zFJ = zFD \frac{c - c'}{\delta} \qquad (7)$$

In this case the cyclic voltammetric performance is strongly influenced by the electrode-electrolyte system. Moreover, as stated by eqn. 7 the current density is proportional to the change of concentration and inversed with the thickness of the diffusion layer. The condition of the diffusion layer such as stirring or convective effects strongly influences the layer thickness and thus, the current density.

FESEM-EDX analysis: For the FESEM study, the present work used a FESEM-ZEISS SUPRA 35 VP provided with a Gemini filed emission column operated at a working distance between 0 mm and 20 nm and at a voltage range between 0.1 kV and 30.0 kV by a 0.1 kV step. A small portion of fabricated ferrite was sputtered on a stub surface and covered by a thin coated platinum. The coated stub surface was placed in a vacuum chamber and was ready for scanning process. Varied magnifications between 10,000x-25,000x were used to obtain representative FESEM images.

An EDX instrument was coupled with the FESEM device and used for determining elemental composition. The EDX analysis performed a spectra of peaks related to the elemental composition making up the specimen being analyzed.

RESULTS AND DISCUSSION

Cyclic voltammetry: This study used a mixture of phosphate buffer and ferricyanide solution, [Fe $(CN)_6]^{3-}$, for the electrolyte system and therefore, a couple of $[Fe(CN)_6]^{3-}/[Fe(CN)_6]^{4-}$ played the redox role in its electrochemical system producing a cyclic voltammogram. The mechanism of the cyclic voltammogram of the $[Fe(CN)_6]^{3-}/[Fe(CN)_6]^{4-}$ couple could be explained as follows. The scan was initiated with $[Fe(CN)_6]^{3-}$ present in solution and, as the potential approached to the standard potential of the couple, the $[Fe(CN)_6]^{3-}$ near the electrode was reduced and current began to flow. As the potential continued to change, the cathodic current began to decline again because all the $[Fe(CN)_6]^{3-}$ near the electrode was reduced and the current reached its limiting value. The potential now returned to linearly to its initial value and the reverse series of events occurred with the $[Fe(CN)_6]^{4-}$ produced during the forward scan now undergoing oxidation. Then, the peak of current performed on the other side, as indicated in the illustration noting by the two peaks. The shape of the cyclic voltammogram can be influenced by the material used for the working electrode. Since fabricated magnesium ferrites with various metal doped (Mn, Co and Ni) were used for the working electrode in this investigation, it was not surprising that various shapes of cyclic voltammograms could be exposed. The results of

this investigation were related to the mechanism proposed by Atkins and Paula[19] involving the type of working electrode used, concentration gradient and diffusion layer.

Fig. 1 showed the cyclic voltammograms of undoped magnesium ferrites at various temperatures of calcinations (400, 500 and 700 °C) at a scan rate of 0.02 V s^{-1}. All reduction peaks appeared to have almost same value of cathodic potentials (H ≈ 0.15 V) as well as their anodic peaks (H ≈ 0.06 V). However, both the cathodic and anodic currents of the various calcined undoped magnesium ferrites (400, 500 and 700 °C) were different in which the 500 °C calcined magnesium ferrite posed the highest cathodic current (7.2 μA) and the highest anodic current (-9.6 μA). The various calcined temperatures caused different atomic distributions and crystalline structures on the surface of working electrode influenced the concentration gradient of the $[Fe(CN)_6]^{3-}/[Fe(CN)_6]^{4-}$ system in the solution (eqn. 4) leading to different current intensities as indicated through eqn. 5 to 7. In this case, it was apparent that the 500 °C calcined magnesium ferrite imposed the best semiconducting properties, thus, the 500 °C magnesium ferrite showed the optimum calcination condition.
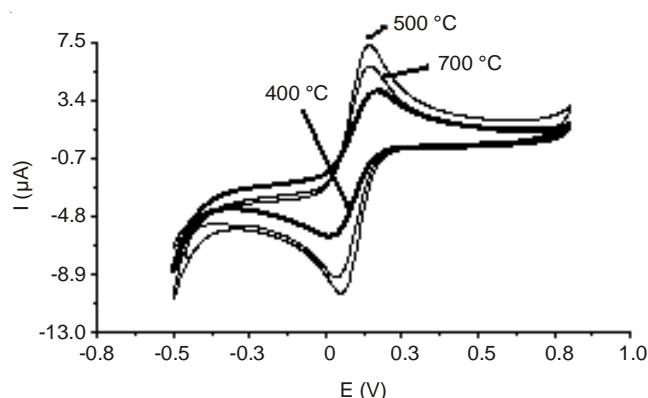
Fig. 1.   Cyclic voltammograms of fabricated magnesium ferrites at various temperatures (400, 500 and 700 °C)

Fig. 2 showed the cyclic voltammograms of cobalt-doped magnesium ferrites (x = 0.1 and 0.9) compared to the undoped magnesium ferrite at the same value of calcined temperature (500 °C). Through the mechanism proposed by Atkins and Paula[19], different cyclic voltammograms performance could be expected. The cathodic peaks of cobalt-doped magnesium ferrites were found to be 0.01 V and 2.6 μA (x = 0.1) and -0.02 V and 7.2 μA (x = 0.9), while the anodic peaks were -0.19 V and -6.0 μA (x = 0.1) and -0.12 V and -9.7 μA (x = 0.9). Regarding the effect of cobalt doping concentration, there were insignificant shifts of both cathodic and anodic potentials, however, a significant increase of cathodic current was observed (2.6 μA to 7.2 μA) when the cobalt doping increased (x = 0.1 to 0.9). A similar phenomenon was also occurred for anodic current (-6.0 μA to -9.7 μA) when the cobalt doping increased (x = 0.1 to 0.9). It appeared that the higher cobalt-doped magnesium ferrite produced better semiconducting properties in this matter. Having a glance look on Fig. 2 as compared to the undoped magnesium ferrite, both the cathodic and anodic currents of cobalt-doped (x = 0.9) were not significantly different from that one of the undoped magnesium ferrite. However,

there was a remarkable shift of the cathodic and anodic potentials to the left side imposed by the cyclic voltammogram of cobalt-doped (x = 0.9) magnesium ferrite. It implies that the cobalt doping (x = 0.9) showed no better impact on the semiconducting properties of the undoped magnesium ferrite. On the other hand, the cobalt-doped (x = 0.1) magnesium ferrite yielded a suppression effect on the semiconducting properties assumed that the atomic distributions in the cobalt-doped (x = 0.1) retarded the mechanism of redox reaction of $[Fe(CN)_6]^{3-}/[Fe(CN)_6]^{4-}$ in the solution.
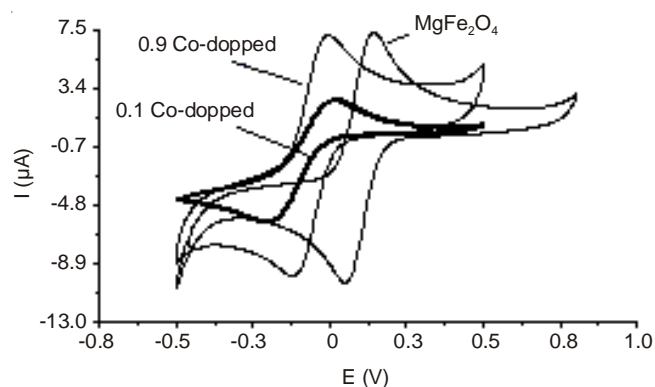
Fig. 2. Cyclic voltammograms of calcined magnesium ferrite, 0.1 Co-doped and 0.9 Co-doped magnesium ferrites calcined at 500 °C

On the other hand, both the nickel-doped magnesium ferrite (x = 0.1 and 0.5) showed a suppression effect of the semiconducting properties as compared to that one of the undoped magnesium ferrite as showed by their cyclic voltammograms in Fig. 3. The electrode potentials of the nickel-doped (x = 0.1 and 0.5) and the undoped magnesium ferrite were not significantly different, but the current intensities of both the nickel-doped (x = 0.1 and 0.5) for the cathodic and anodic peaks posed a significant reduction compared to that one of the undoped magnesium ferrite. It implies that the nickel doping did not enhance the semiconducting properties of magnesium ferrite.
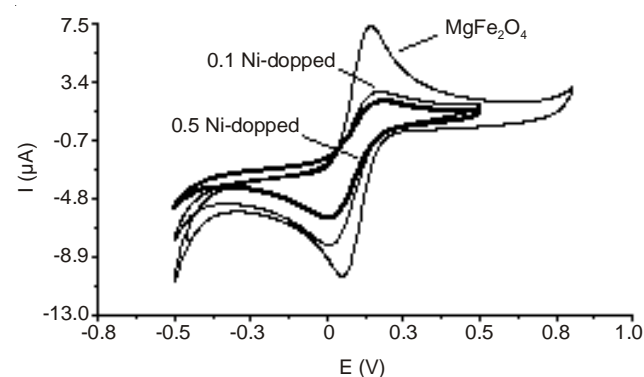
Fig. 3. Cyclic voltammograms of magnesium ferrite, 0.1 Ni-doped and 0.5 Ni-doped magnesium ferrites calcined at 500 °C

Fig. 4 showed the cyclic voltammograms of different metal doped in magnesium ferrite (Mn, Co and Ni). At the same value of scan rate (0.02 V s⁻¹), the redox reaction of $[Fe(CN)_6]^{3-}/[Fe(CN)_6]^{4-}$ using the cobalt-doped magnesium ferrite (x = 0.5) indicated by the broader cyclic voltammogram took longer

time than that one using the manganese-doped (x = 0.5). It was apparent that the cobalt-doped magnesium ferrite (x = 0.5) produced a retardation effect on the redox reaction of $[Fe(CN)_6]^{3-}/[Fe(CN)_6]^{4-}$. Unfortunately, the mechanism of this phenomenon is still unclear. Compared to the cyclic voltammograms of both cobalt-doped and manganese-doped magnesium ferrites, the nickel-doped magnesium ferrite yielded lower current intensity for both cathodic and anodic currents at the same value of doping concentration (x = 0.5). The different performance of cyclic voltammograms produced by different metal doping (Mn, Co and Ni) in the fabricated magnesium ferrite used for working electrode is apparently related to the different electronic rearrangement in the *3d* sub shell of those transition metals. In the study of morphology and composition of electrodeposited Zn-Ni alloys, Abou Krisha *et al.*[3] reported that different phases in Zn-Ni alloys produced different shifts of anodic potentials in the cyclic voltammograms. Different materials such as a bare glass carbon electrode (GCE), TiO₂/ GCE, MWCNT/GCE and MWCNT/TiO₂/GCE separately used for working electrodes produced different performance of cyclic voltammograms as reported by Ganchimeg *et al.*[6] in the study of ascorbic acid oxidation. Moreover, Ganchimeg *et al.*[6] found that the oxidation peaks in the cyclic voltammograms reduced with the following order of MWCNT/TiO₂/GCE, MWCNT/ GCE, bare GCE and TiO₂/GCE. On other occasions, Lawal and Wallace[4] found that doubled the concentration of nafion dopant used for platinum coating increased its cathodic and anodic currents at the same value of current density (5 mA cm⁻²) and there was a shift of cathodic potential to the right side. It seems that this study is consistent with the previous investigations in terms of type and concentration of metal doped ferrites used for working electrodes. This study regarding the cyclic voltammograms in relation to types of metal doping and doping concentration in the fabricated magnesium ferrite gives valuable information for further investigation on semiconducting properties and electrochemical behaviour particularly for ferrite material.
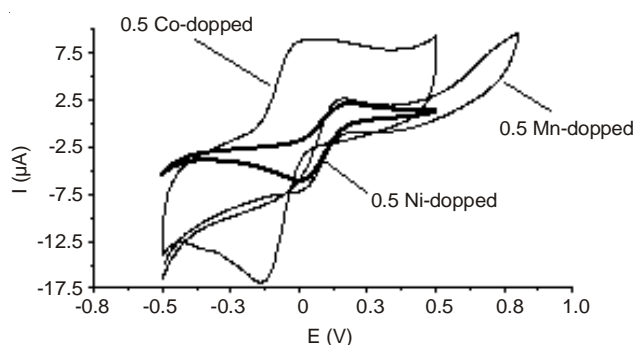
Fig. 4. Cyclic voltammograms of 0.5 Mn-doped, 0.5 Co-doped and 0.5 Ni-doped magnesium ferrites at 500 °C

FESEM-EDX analysis: The FESEM images indicated the morphology of surface structures of the ferrite and its corresponding metal doped caused by electrons bombardment onto the surface of a material. The FESEM micrograph was provided by EDX spectra to inform the elemental analysis of the corresponding surface. Fig. 5a showed the FESEM micrograph of magnesium ferrite calcined at 500 °C. The scattered
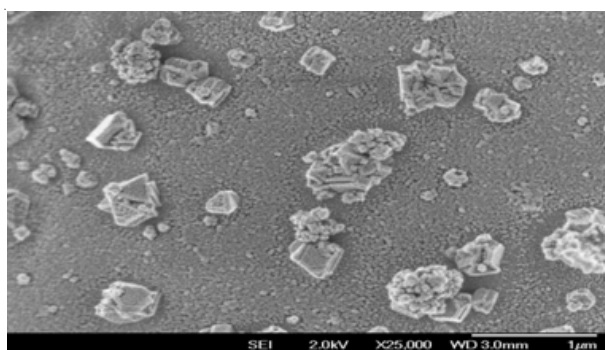
Fig. 5a. FESEM micrograph of magnesium ferrite calcined at 500 °C with toping of Fe_3O_4 cubic crystals

granular particles shown in the micrograph indicated the cubic structure of Fe_3O_4. The structure of Fe_3O_4 was supported by the XRD data (not shown here) as presented by the remarkable peaks of 311 and 440 at respective $2\theta = 35°$ and $63°$. The investigation of magnesium ferrite using a sol gel route reported by Pradeep et al.[10] showed a similar pattern as that one of this study, which indicated the presence of Fe_3O_4 in addition to the $MgFe_2O_4$. The EDX analysis (Fig. 5b) showed the elemental composition of the corresponding undoped ferrite surface calcined at 500 °C.
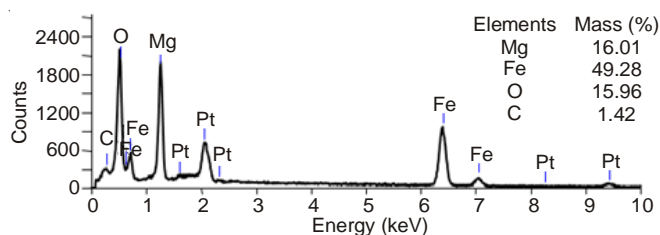
Fig. 5b. EDX spectra of magnesium ferrite calcined at 500 °C

Fig. 6a showed the FESEM micrograph of Co-doped magnesium ferrite (x = 0.1) calcined at 500 °C. The scattered granular particles shown in the micrograph was assumed to contain cobalt atoms as indicated by the elemental data of EDX analysis (Fig. 6b).
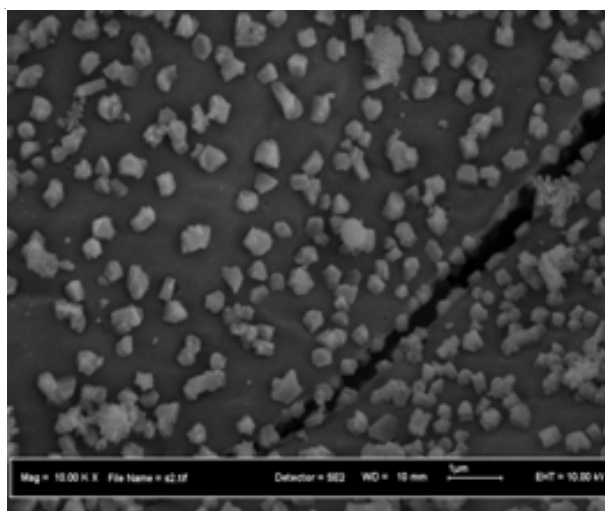
Fig. 6a. FESEM micrograph of 0.1 Co doped magnesium ferrite calcined at 500 °C with toping of Fe_3O_4 cubic crystals
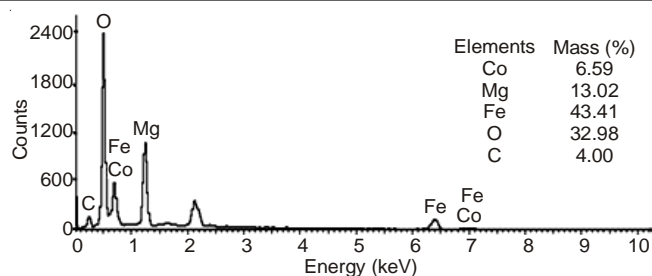
Fig. 6b. EDX spectra of 0.1 Co-doped magnesium ferrite calcined at 500 °C

Pradeep and Chandrasekaran[9] using a sol gel route for the synthesis of metal doped magnesium ferrite (Ni, Cu and Zn) investigated the XRD analysis in terms of lattice constant and particle size of the bimetal ferrites. Moreover, the theory of Pradeep and Chandrasekaran[9] proposed the metal doped occupied together with magnesium and iron(III) in the lattice site of $M_xMg_{1-x}Fe_2O_4$ (M = Ni, Cu and Zn) either in tetrahedral or octahedral structure. It is possible that the cobalt doped magnesium ferrite in this study occupied together with magnesium and iron(III) in the lattice site of $Co_{0.1}Mg_{0.9}Fe_2O_4$. Elemental substitution between cobalt and iron ions is likely to occur rather than that one between cobalt and magnesium ions because the atomic numbers of cobalt and iron are closer. Moreover, the cubic crystalline of the scattered granular particles in the FESEM micrograph (Fig. 6a) was assumed partly belongs to Fe_3O_4. Regarding the EDX analysis, the concentration of oxygen (H ≈ 33 %) in the cobalt doped magnesium ferrite (x = 0.1) as shown in Fig. 6b is roughly doubled the concentration of oxygen in undoped magnesium ferrite (H ≈ 16 %) as shown in Fig. 5b. It was apparent that the presence of cobalt caused the resistance of oxygen removal from the surface part, which was expected to the bonding formation between cobalt and oxygen. In addition, the reduction in concentrations of both magnesium (from 16 to 13 %) and iron (from 49 to 43 %) obtained from the EDX analyses (Figs. 5b and 6b) was assumed due to the presence of cobalt. The cobalt ions partly replaced the position of magnesium and iron ions in the lattice site of $Co_{0.1}Mg_{0.9}Fe_2O_4$. The study of FESEM provided with EDX analysis is useful to examine the atomic distribution on the ferrite surface in relation to its electrochemical behaviour. Furthermore, the morphology of crystalline structure obtained from FESEM-EDX analysis gives valuable contribution to explain the semiconducting properties of ferrites.

Conclusion

The cyclic voltammetry of the screen printed carbon working electrode covered by fabricated undoped and metal doped ferrites (Mn, Co and Ni) dipped in a solution of $[Fe(CN)_6]^{3-}/[Fe(CN)_6]^{4-}$ and phosphate buffer produced different performances in terms of alteration on cathodic and anodic currents in relation to shifting of electrode potential due to different electrochemical behaviours. The types of metal doping and doping concentration yielded different presentations of cyclic voltammograms influenced by the mechanism involving the concentration gradient, diffusion layer and flux of charge transfer. The redox characteristic influenced the diffusion rate as the rate limiting step and could lead to the redox reaction rate. Therefore, this study gives valuable contribution for the application of ferrites and their metal doped in a broader sense.

REFERENCES

1. S. Maensiri, M. Sangmanee and A. Wiengmoon, *Nanoscale Res. Lett.*, **4**, 221 (2009).
2. M. Siemons, Th. Weirich, J. Mayer and U. Simon, *J. Inorg. General Chem.*, **630**, 2083 (2004).
3. M.M. Abou-Krisha, A.M. Zaky and A.A. Toghan *Asian J. Biochem.*, **1**, 84 (2006).
4. A.T. Lawal and G.G. Wallace, *J. Appl. Sci.*, **8**, 2967 (2008).
5. M. Hayyan, F. S. Mjalli, M.A. Hashim, I. M. Al-Nashe, X.M. Tan and K.L. Chooi, *J. Appl. Sci.*, **10**, 1176 (2010).
6. P. Ganchimeg, W.T. Tan, N.A. Yusof and J.K. Goh, *J. Appl. Sci.*, **11**, 848 (2011).
7. L.D.Lick, and D.B. Soria, *J. Argentine Chem. Soc.*, **97**, 102 (2008).
8. P. Puspitasari, N. Yahya, N.A.M. Zabidi and N.A. Ahmad, *J. Appl. Sci.*, **11**, 1199 (2011).
9. A. Pradeep and G. Chandrasekaran, *Mater. Lett.*, **60**, 371 (2006).
10. A. Pradeep, P. Priyadharsini and G. Chandrasekaran, *J. Magn. Magn. Mater.*, **320**, 2774 (2008).
11. H. Abdullah, R. Silvia and J. Syarif, *Asian J. Appl. Sci.*, **2**, 191 (2009).
12. N. Yahya, M. Akhtar, A.F. Masuri and M. Kashif, *J. Appl. Sci.*, **11**, 1303 (2011).
13. P. Arsana, C. Bubpa and W. Sang-aroon, *J. Appl. Sci.*, **12**, 1809 (2012).
14. A.S. Juarez, C.E. Benouis and M.S. Aida, *J. Appl. Sci.*, **7**, 220 (2007).
15. U.R. Mazhar, I. Misbah-ul and A. Tahir, *Pakistan J. Appl. Sci.*, **2**, 1110 (2002).
16. A.A. Sattar, H.M. El-Sayed, K.M. El-Shokrofy and M.M. El-Tabey, *J. Appl. Sci.*, **5**, 162 (2005).
17. M.G. Naseri, E.B. Saion, H.A. Ahangar, M. Hashim and A.H. Shaari, *J. Magn. Magn. Mater.*, **323**, 1745 (2011).
18. A. Reguig, M.M. Mostafa, L. Larabi and Y. Harek, *J. Appl. Sci.*, **8**, 3191 (2008).
19. P. Atkins and J. Paula, Physical Chemistry, Oxford University Press, edn 7, pp. 1031-1035 (2002).